Towards Accurate Computations of Active Stabiliser Fins, focusing on Dynamic Stall

Gerson Fernandes, *MARIN Academy,* gcf105@yahoo.com
Geert Kapsenberg, *MARIN,* G.K.Kapsenberg@marin.nl
Maarten Kerkvliet, *MARIN,* M.Kerkvliet@marin.nl
Frans van Walree, *MARIN,* F.v.Walree@marin.nl

ABSTRACT

Steps towards accurate and efficient characterisation of the hydrodynamic behaviour of active stabiliser fins have been conducted using computational fluid dynamics. Conditions seen at hydrodynamic testing facilities (Reynolds number = 135,000), with an angle of attack variation described as $\alpha(t) = 10° + 15° \sin(\omega t)$ have been modelled in two dimensions with various RANS turbulence models (k-ω SST, k-√kl, Spalart-Allmaras & LCTM) for reduced frequencies k=0.1 & 0.05. Solutions were compared to experimental results and results from other calculation methods (LES) and to results from a typical sea keeping code. The results showing the hysteresis loop for C_L and C_D show that a good agreement was seen to the literature. For seakeeping applications, moderate refinement in time and space is sufficient, and that the k-ω SST turbulence model best matches the C_L and C_D curves found in the literature. The increased knowledge of stabiliser fins dynamics will be used to improve time-domain seakeeping codes and possible also the control laws for active stabilizer fins.

Keywords: *Active stabiliser fins; Dynamic stall; Computational fluid dynamics; RANS turbulence models; Roll damping*

1. INTRODUCTION

The subject of roll damping is an engineering topic with active research, and is important for a wide range of ship types, affecting not only the cargo but also the comfort and safety of the passengers and crew on board. The problem originates from the lack of inherent roll damping from a bare hull, and is compounded by the dominant importance of viscous effects (Wang et al. 2012)(Bačkalov et al. 2015). To overcome this deficiency, devices such as bilge keels, anti-roll tanks, for example, can be employed. Alternatively, stabilizer fins can also be used, where an appropriately mounted fin is used to produce a roll restoring moment. Furthermore, stabilizer fins can be passive or active; the latter consist of moving surfaces as a component of a control system. Typically, the fin operates by changing the angle of attack, and can enter the dynamic stall regime. Dynamic stall occurs when a lifting surface is subject to a sufficiently large variation of the angle of attack, (Leishman 2006). Towing tank experiments (Gaillarde 2003) have shown that the dynamic stall angle by far exceeds the static value. This result was a strong motivation for this study.

The subject of dynamic stall presents a set of challenges on its own. This was studied in the context of helicopter blades for example by (McCroskey, Carr, and McAlister 1976), with its own and distinct Reynolds (Re) and Mach number regime. Less attention has been given to the Reynolds regime of order 100,000 but comparatively recently, two investigations stand out. A study by (Lee and Gerontakos 2004), concerned low-speed wind tunnel experiments for a NACA 0012 section at Reynolds number=135,000. Secondly, (Kim and Xie 2016) conducted thorough Large Edge Simulations (LES) for the same geometry, where a good agreement was seen to the experiments and further, the influence of free-stream turbulence was assessed. Other results performed with RANS models include (Wang et al. 2012) and (Gharali and Johnson 2013), where in general the maxima and minima and overall hysteresis loop for the force coefficients agree with the experimental results. However, the force coefficients show large oscillations, particularly on the down stroke.

The work presented here will detail numerical simulations performed with computational fluid

dynamics (CFD) code for conditions seen at hydrodynamic wind/wave testing facilities of an isolated stabilizer fin section. Given the difficulties forecasted in the literature, a careful and progressive approach will be adopted. Two reduced frequencies will be tested and compared to the literature and a typical seakeeping code.

The end objective of this work is to improve the knowledge of the stall of stabiliser fins, with particular emphasis on improving current seakeeping codes, which currently model poorly the behaviour at high angles of attack and hysteresis.

2. METHODOLOGY

ReFRESCO

The numerical simulations performed with CFD code described in (ReFRESCO), a viscous-flow code that solves the incompressible Navier-Stokes equations. This finite-volume code uses a cell-centred approach and the SIMPLE pressure-correction equation for mass conservation. Time stepping is performed implicitly with a second-order backward scheme. Turbulence models are used in a segregated approach, and include the k-ω SST (Menter and Langtry 2003), k-√kl (Menter, Egorov, and Rusch 2006), Spalart-Allmaras (Aupoix and Spalart 2003) and the LCTM (Langtry and Menter 2009).

Geometry, Grid Generation & Boundary Conditions

The fin section was assumed to be a NACA 0012. This symmetrical airfoil has been the subject of several numerical and experimental investigations. The analytical equations describing this airfoil have been closed, resulting in a rounded trailing edge with a small radius (0.125% of the chord). The computational domain is discretised using the commercial software GridPro. The resulting structured mesh had a circular far field of 100 chords radius (from a domain size study), as boundary related issues were beyond the current scope. The entire boundary layer was resolved, and therefore a y^+,

$$y^+ = u_* y / v \quad (1)$$

(where u_*: friction velocity and v: kinematic viscosity) value of < 1 was required. This is done to correctly remove the necessity of employing wall functions. Boundary conditions were such that an inflow and outflow boundaries were present at the extremes of the domain, and a pressure condition above and below (see schematic in Figure 1). Two dimensionality was ensured using symmetry boundaries on the sides. Five geometrically similar grids, ranging from 368-56k cells were tested (see Figure 2).

Two grid motion methods have been tested, a rigid grid motion and grid deformations using a radial basis function, where no appreciable difference was seen. The target iterative convergence, an important metric when performing CFD results, was set to 1E-5 in the L_{INF} (worst case). Typically, the RMS (L_2 norm) residual value is 1-2 orders lower.

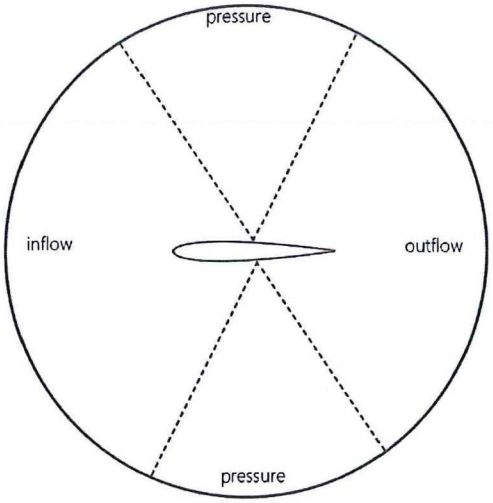

Figure 1: Boundary condition schematic

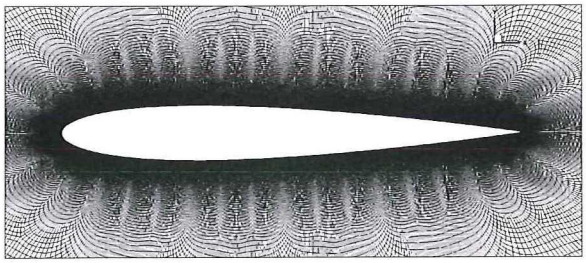

Figure 2: Mesh around the NACA 0012 section

PanShip

Results were also compared to PanShip (Walree 2002), a typical seakeeping code. PanShip is an unsteady time domain boundary element method for ships equipped with (or without) lifting surfaces for motion control. Linearised free surface effects are incorporated through the use of transient Green functions. Lifting surfaces are discretised in to quadrilateral panels with a constant source and doublet strength. Wake sheets consisting of doublet

panels emerge from the trailing edge. Viscosity effects are approximated by using empirical formulations for frictional resistance and drag due to flow separation.

Flow conditions and Fin Section Kinematics

Flow conditions typically seen in towing tanks have been modelled, and given the availability of the literature, the Reynolds number is chosen as:

$$Re = \frac{\rho U_\infty c}{\mu} = 135{,}000 \qquad (2)$$

where ρ: density, U_∞: inlet velocity, c: chord length & μ: dynamic viscosity.

The prescribed fin motions are described as:

$$\alpha(t) = \alpha_{mean} + \alpha_{amp}\sin(\omega t) \qquad (3)$$

The mean angle of attack (α_{mean}) was 10° and the amplitude of oscillation ($\alpha_{amp} = \pm 15°$).

The frequency of oscillation is non-dimensionalised in the reduced frequency,

$$k = \frac{\omega c}{2U_\infty}. \qquad (4)$$

Two reduced frequencies were tested, 0.1 & 0.05. The force coefficients are normalised with respect to the chord length, inlet velocity, α_{mean} and planform area.

3. RESULTS, *k*=0.1

Iterative convergence

A typical iterative convergence is shown in Figure 3, where also the C_L and angle of attack can be seen (including a starting up transient). The force signal is seen to be periodical; no signal processing has been performed of the presented force coefficient signals. The LES results are phase averaged over 3 cycles and the experiments over 100 cycles, which could explain the smoothness of the results. It is seen how part of the cycle of oscillation does not meet the target iterative convergence, and that these time steps are near the maximum incidence, where the flow is very complex and therefore numerically more difficult to solve. An effort was made to further improve the convergence, but no appreciable difference was seen in the force signal. Hence, the current shown results presented are deemed to be sufficiently converged.

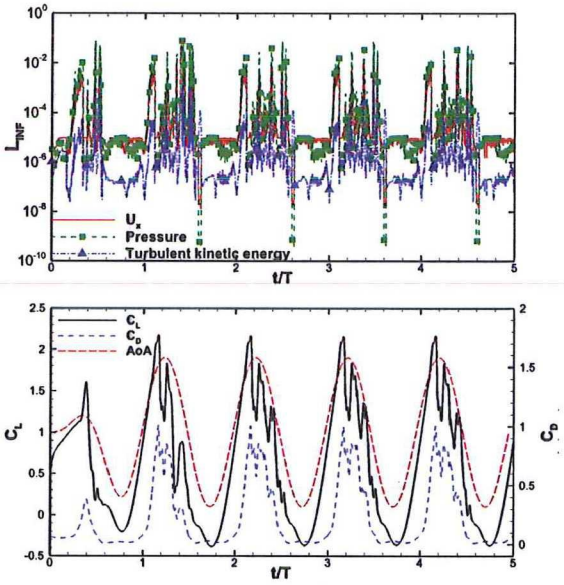

Figure 3: Typical convergence for U_x, pressure & turbulent kinetic energy equations (upper figure) and C_L signal (lower figure). Reduced frequency, k=0.1; turbulence model: k-ω SST; time step, T/dt=800.

Turbulence Model

The force coefficients for all the tested turbulence models against the AoA are shown in Figure 4-6 below for all the tested turbulence models. The upstroke has a very different behaviour compared to the down stroke, where, different to the smooth slope on the upstroke, the down stroke shows several oscillations. These oscillations correspond to the shedding of vortices, and given the inherent differences in the turbulence models, this results in a different shedding strength and location. The peak C_L values are comparable for all turbulence models and agree well with the LES, but are approximately 8% lower than the experiments. A detailed discussion and possible explanation for this mismatch is given in (Kim 2013). The LCTM model does account for laminar-turbulent boundary layer transition, but no appreciable difference is seen for this case. Given the current reduced frequency, it is likely that inertial effects dominate the viscous phenomena, such as boundary layer transition. Comparing to the LES, it appears that the k-ω SST model better captures the down stroke behaviour. When oscillations in the C_L occur, the values are also higher than predicted by the LES. This over prediction could be explained by the two-dimensional nature of the current CFD simulations. Similarly, the C_D curve shows a good agreement between all the RANS models.

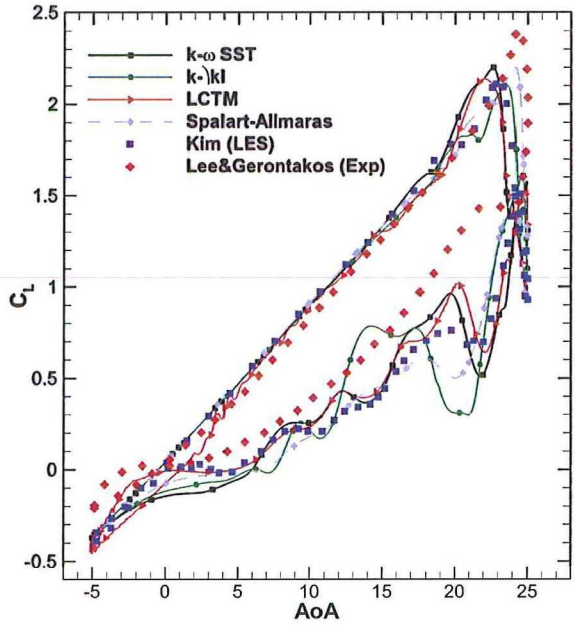

Figure 4: C_L vs AoA for the various turbulence models

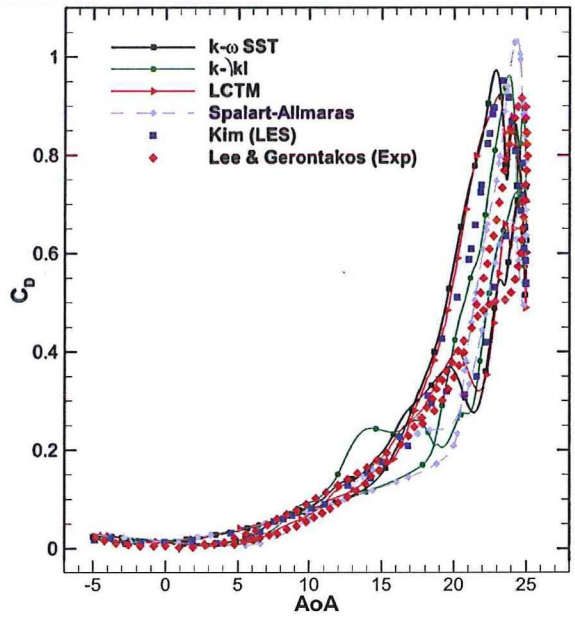

Figure 5: C_D vs AoA for the various turbulence models

Time step refinement

Given the unsteady nature of the problem, it is important to assess the sensitivity of the force coefficients on the time step. Four time steps have been tested with the k-√kl model, and the effect on the C_L is shown in Figure 6. It can be seen that during the upstroke (-5→25 degrees), no significant influence of the time step is seen (this is also evident by the easier convergence, see Figure 3). However, during the down stroke (25→-5 degrees), relatively small differences in amplitude are seen, and are essentially identical when the incidence returns to approximately -5 degrees. These differences are again attributed to the shedding of the vortices, but are not of primary interest for a seakeeping context and therefore a value of $T/dt = 400$ (T: period of oscillation), will suffice.

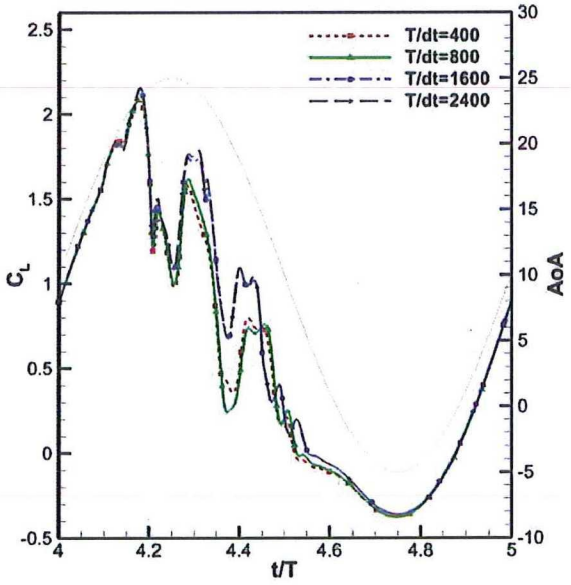

Figure 6: C_L vs t/T for various time steps (k-√kl model, finest grid). Incidence also shown (right axis)

Grid Refinement

The five geometrically similar grids have been tested, and are shown below in Figure 7-8 (see figure caption for legend information). Some relevant grid parameters are shown in Table 1 (see caption for details). The flow can again be divided into two distinct motions, the up and down stroke. The coarsest grid loses much of the detail comparing to the other grids, showing a smoother profile. Apart from the coarsest grid, all grid densities show a good agreement of the C_L vs AoA to the LES. The peak C_L and its associated AoA are also in agreement. Again, the main differences are seen during the down stroke, where the coarsest grid loses much of the detail seen in the finer grids. The C_D is in good agreement for all grid densities.

Grid	Cells	$y^+\|_{max}$	$\overline{y^+\|_{max}}$	Max. C_L	Max. C_D
A	368E3	0.42	0.24	2.18	1.00
C	187E3	0.57	0.35	2.16	0.941
E	104E3	0.69	0.44	2.15	0.927
G	56E3	1.0	0.6	2.26	0.952

Table 1: Summary of grid refinement study. Showing number of cells, maximum y^+ found in the cycle, the phase averaged maximum y^+, and the maximum C_L and C_D.

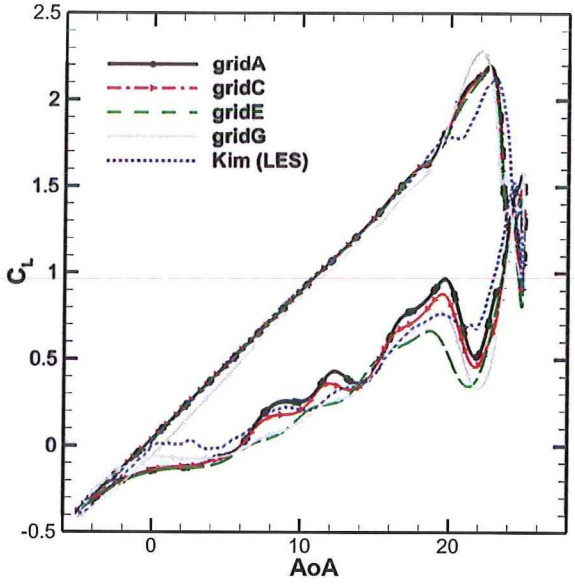

Figure 7: C_L vs AoA for different grid densities, k-ω SST turbulence model. Note grid denoted "A" is the finest (368k cells) and "G" is the coarsest (56k cells)

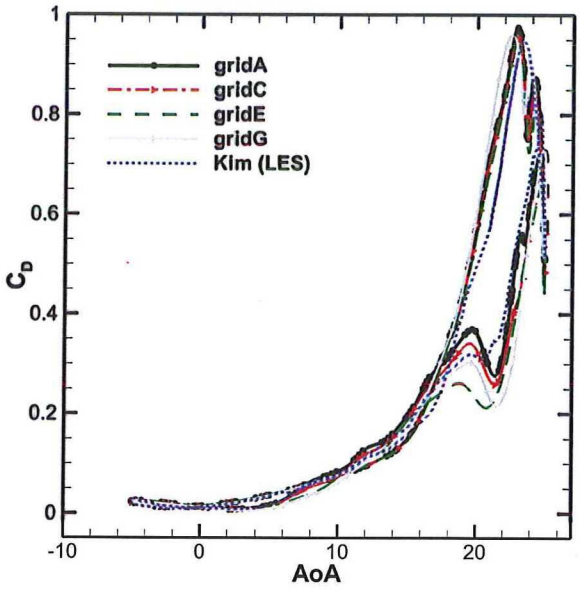

Figure 8: C_D vs AoA for different grid densities. See previous figure for legend information

Discussion & comparison with PanShip

The comparison of the ReFRESCO results with results from literature and with PanShip results is shown in Figure 9. ReFRESCO results show that stall is adequately captured. The sharp decrease in force (from about 2.2 to 0.5 for the C_L) between 20 degrees on the up and down stroke compares well to published data. This decrease is of practical engineering importance, indicating how quickly the fin loses a large portion of the generated lift force. It is also shown that between approximately 0 degrees on the down stroke and 0 degrees on the upstroke, no hysteresis effect is observed. This compares to the LES, while the experiments predict a small hysteresis effect at this portion of the cycle. PanShip can predict the maximum and minimum C_L, and the upstroke behaviour, as well as some hysteresis. The largest difference is seen on the down stroke, where the complex system of vortices is inherently not accounted for. The enclosed area (a measure of the work done) between up and down strokes is also much smaller. The notable decrease in force mentioned above is also not captured.

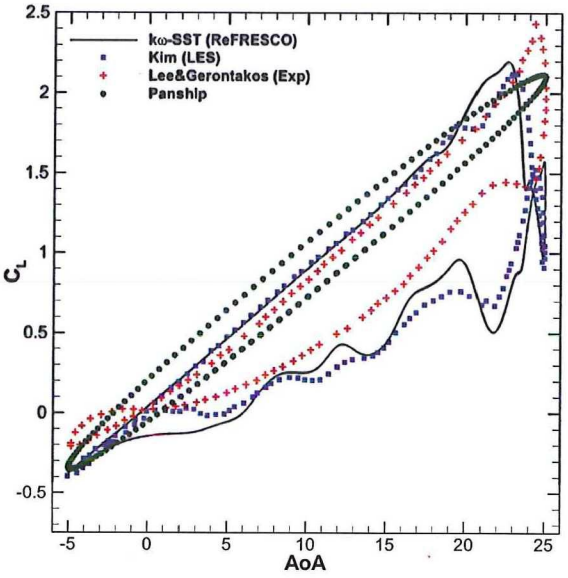

Figure 9: C_L vs AoA, comparison with PanShip

The maximum C_D shows an under prediction of close to 50% compared to all the other results, and is higher at the minimum AoA. Again, some hysteresis is present.

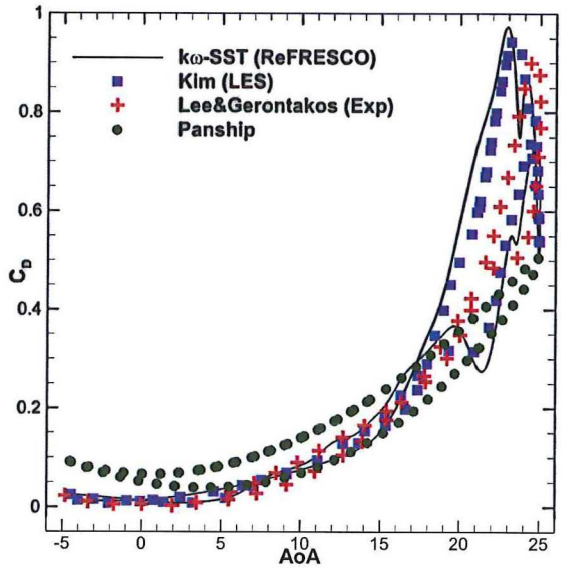

Figure 10: C_D vs AoA, comparison with PanShip

4. RESULTS, k=0.05

A lower reduced frequency (and therefore slower rotation velocity) has been performed for k=0.05. The comparison of force coefficients between ReFRESCO, literature and PanShip is shown in Figure 11 and Figure 12. The current ReFRESCO results appear to over predict the maximum C_L and C_D by 19% and 21.4% respectively (see "flow field description" below for further discussion). With exception of the peak value, a good agreement is seen for both for force coefficients. Another difference captured by the current ReFRESCO results are the oscillations seen on the down stroke, which are not present in the literature. The solution obtained is periodical, and in the figures below 4 cycles are plotted, and practically no differences are observed between the cycles.

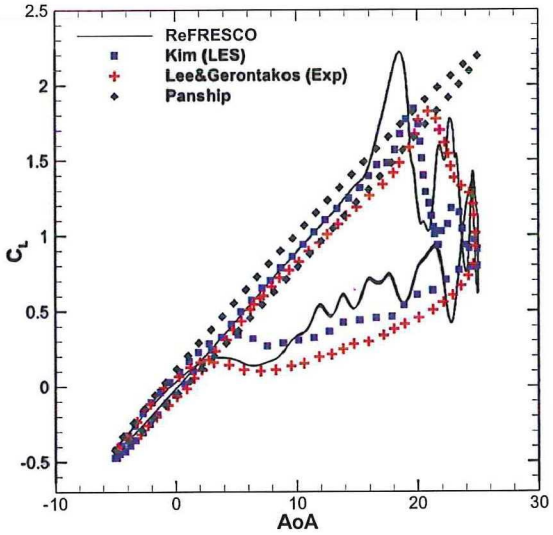

Figure 11: C_L vs AoA, k=0.05

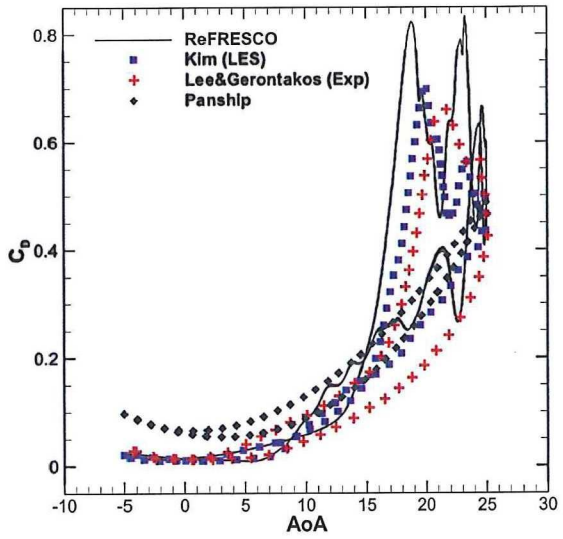

Figure 12: C_D vs AoA, k=0.05

Contrasting with the higher reduced frequency, it can be seen that between approximately 5 degrees on the down stroke and upstroke, no influence of the hysteresis is observed (comparing to 0 degrees for k=0.1).

Flow field description

The flow field is shown in Figure 13, coloured by the non-dimensional stream wise velocity (U_x/U_∞) contours (see caption for details). The calculated peak in C_L and C_D that is not seen in the other results is the result from an over prediction of the negative pressure of the suction side. Once this dominant vortex has been shed, the forces compare better to the LES results.

From the flow field it can also be seen how the oscillations in the force coefficients arise from the shedding of vortices and that the predominant vortex results from the leading edge vortex. The complex flow field also highlights the complexity of the flow, consisting of leading and trailing edge shear layers, bluff-body like shedding from the fin section and adynamic wake. For k=0.05, the maximum C_L occurs at ~19°.

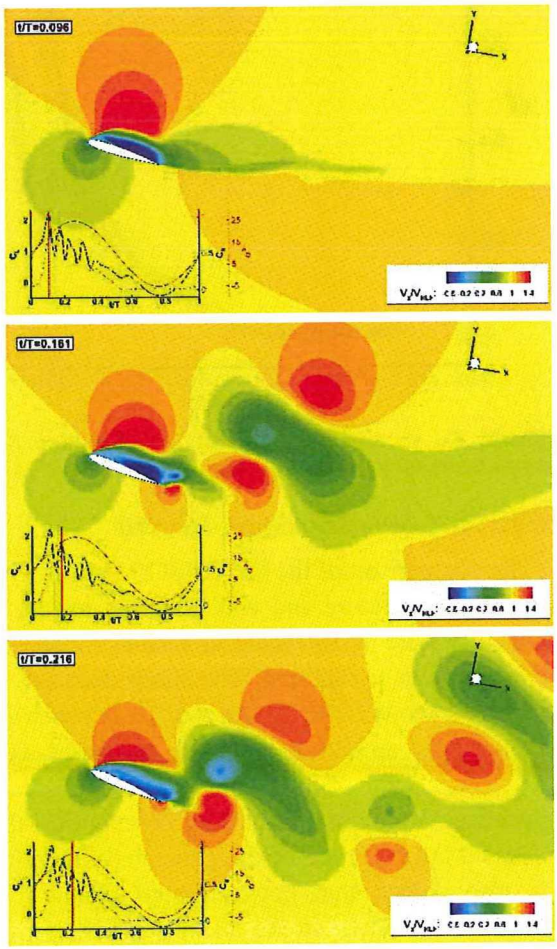

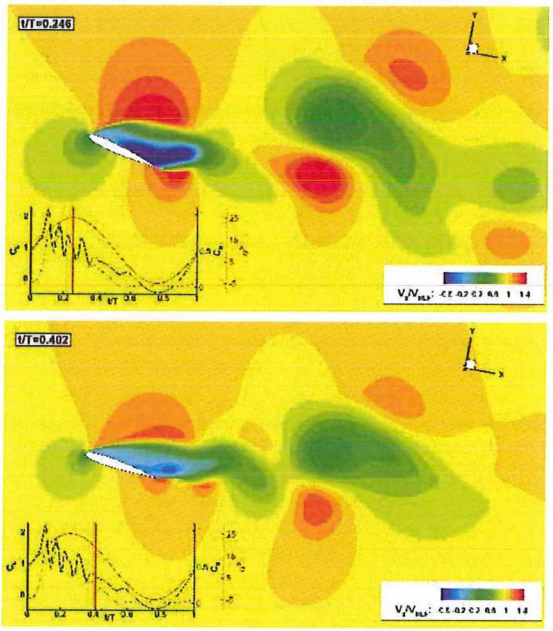

Figure 13: Flow field (stream wise/inlet velocity ratio) showing differing portions of the pitching cycle. 18.6° upstroke; 22.8° upstroke; 24.7° upstroke; maximum AoA, 25°; first down stroke oscillation, 18.7° down stroke

5. CONCLUSIONS

The flow around an stabilizer fin section performing an harmonically oscillating motion has been calculated using CFD. The sensitivity to different RANS turbulence models, time steps and grid refinements have been studied and recommendations are made for these settings assuming the current engineering context. Periodical solutions were obtained for all cases. The iterative convergence was monitored, and the boundary layer resolved at all time steps. Results were compared to literature, where overall a good agreement was found. Specifically, the maximum and minimum values for C_L and C_D (in particular for k=0.1) and the upstroke profile of the force coefficients compared well to published results. For k=0.05, peak values are over predicted by ~20% compared to the literature. The oscillations seen on the force coefficients of the down stroke are attributed to the complex system of vortices present, and are visualised by contour plots. Comparison to a typical seakeeping code shows the big improvement in correctly predicting the stalling behaviour of the fin section. The upstroke behaviour is comparable between the seakeeping code and the CFD, but the classical method vastly under estimates the effect of the stalling behaviour on the down stroke.

6. FURTHER WORK

Further work will be done to incorporate the obtained knowledge on the dynamic stall effect for seakeeping applications. Two methods are currently being assessed, either using a database calculated a-priori, or a robust coupling between the CFD code and the seakeeping tools.

7. ACKNOWLEDGEMENTS

The authors are grateful to Dr. Yusik Kim and the Aerodynamics and Flight Mechanics (AFM) group of the University of Southampton for their valuable comments and making their data available.

8. REFERENCES

Aupoix, B., and P.R. Spalart. 2003. "Extensions of the Spalart–Allmaras Turbulence Model to Account for Wall Roughness." *International Journal of Heat and Fluid Flow* 24(4): 454–62.

Bačkalov, Igor et al. 2015. "Ship Stability, Dynamics and Safety: Status and Perspectives." In *12th International Conference on the Stability of Ships and Ocean Vehicles*, Glasgow, UK.

Gaillarde, Guilhem. 2003. "Dynamic Stall and Cavitations of Stabilizer Fins and Their Influence on the Ship Behaviour." In *FAST*, Napels.

Gharali, Kobra, and David a. Johnson. 2013. "Dynamic Stall Simulation of a Pitching Airfoil under Unsteady Freestream Velocity." *Journal of Fluids and Structures* 42: 228–44. http://dx.doi.org/10.1016/j.jfluidstructs.2013.05.005.

Kim, Yusik. 2013. "Wind Turbine Aerodynamics in Freestream Turbulence." University of Southampton.

Kim, Yusik, and Zheng-Tong Xie. 2016. "Modelling the Effect of Freestream Turbulence on Dynamic Stall of Wind Turbine Blades." *Computers & Fluids* 129: 53–66.

Langtry, Robin B., and Florian R. Menter. 2009. "Correlation-Based Transition Modeling for Unstructured Parallelized Computational Fluid Dynamics Codes." *AIAA Journal* 47(12): 2894–2906.

Lee, T., and P. Gerontakos. 2004. "Investigation of Flow over an Oscillating Airfoil." *Journal of Fluid Mechanics* 512: 313–41.

Leishman, J. G. 2006. Cambridge Aerospace Series *Principles of Helicopter Aerodynamics*. New York: Cambridge University Press.

McCroskey, W. J., L. W. Carr, and K. W. McAlister. 1976. "Dynamic Stall Experiments on Oscillating Airfoils." *AIAA Journal* 14(1): 57–63.

Menter, F. R., Y. Egorov, and D. Rusch. 2006. "Steady and Unsteady Flow Modelling Using the K-skL Model." *Proceedings of the International Symposium on Turbulence, Heat and Mass Transfer*: 403–6.

Menter, F. R., and M. Langtry. 2003. "Ten Years of Industrial Experience with the SST Turbulence Model." In *Fourth International Symposium on Turbulence, Heat and Mass Transfer*, eds. K. Hanjalic, Y. Nagano, and M. Tummers. Ankara, Turkey.

"ReFRESCO." www.refresco.org.

Walree, F Van. 2002. "Development, Validation and Application of a Time Domain Seakeeping Method for High-Speed Craft with a Ride Control System." In *24th Symposium on Naval Hydrodynamics*, Fukuoka, Japan.

Wang, Shengyi et al. 2012. "Turbulence Modeling of Deep Dynamic Stall at Relatively Low Reynolds Number." *Journal of Fluids and Structures* 33: 191–209.